

## Article

# Optimization of the Preparation of Hydrophilic Poly(DHPMA-co-MBA) Monolithic Capillary Columns: A New Support for Affinity Chromatography

Julie Gil, Gaëtan Passalacqua, Adrien Deloche, François-Xavier Vidal, Vincent Dugas \*  and Claire Demesmay

Institut des Sciences Analytiques, Université Claude Bernard Lyon 1, ISA UMR 5280, CNRS, 5 rue de la Doua, 69100 Villeurbanne, France; julie.gil@univ-lyon1.fr (J.G.); gaetan.passalacqua@etu.univ-lyon1.fr (G.P.); francoisxaviervidal@live.fr (F.-X.V.); demesmay@univ-lyon1.fr (C.D.)

\* Correspondence: vincent.dugas@univ-lyon1.fr

**Abstract:** In miniaturized affinity chromatography, the development of hydrophilic organic monoliths with reduced non-specific interactions and high-protein grafting capacity remains a hot topic. In this work, we propose the one-step synthesis of a diol organic monolith to replace the gold-standard epoxy-based organic monoliths (which require post-modification, namely hydrolysis, prior to use). The synthesis of this new monolith builds upon the use of N-N'-Methylenebis(acrylamide) (MBA), as a hydrophilic crosslinker, and 2,3-dihydroxypropyl methacrylate (DHPMA), a diol monomer that eliminates the time-consuming epoxy ring opening step and its associated side reactions. The optimization of one-step synthesis parameters led to a monolith with a satisfactory permeability ( $(4.8 \pm 0.5) \times 10^{-14} \text{ m}^2$ ), high efficiency (117,600 plates/m at optimum flow velocity ( $u_{\text{opt}} = 0.09 \text{ cm s}^{-1}$ )) and reduced non-specific interactions. It is exemplified by its separation ability in the HILIC mode (separation of nucleosides), and by the retention data set of 41 test solutes, which were used to evaluate the non-specific interactions. This new poly(DHPMA-co-MBA) monolith has not only hydrophilic surface properties, but also improved protein grafting capacity compared to the glycidyl-based monolith ( $13 \pm 0.7 \text{ pmol cm}^{-1}$ ). The potential of this monolith is illustrated in affinity chromatography, where the concanavalin ligands are ranked according to their  $K_d$  values.

**Keywords:** monolith; capillary liquid chromatography; HILIC; non-specific interactions



**Citation:** Gil, J.; Passalacqua, G.; Deloche, A.; Vidal, F.-X.; Dugas, V.; Demesmay, C. Optimization of the Preparation of Hydrophilic Poly(DHPMA-co-MBA) Monolithic Capillary Columns: A New Support for Affinity Chromatography.

*Separations* **2023**, *10*, 437.

<https://doi.org/10.3390/separations10080437>

Academic Editor: Victoria Samanidou

Received: 29 June 2023

Revised: 25 July 2023

Accepted: 30 July 2023

Published: 2 August 2023



**Copyright:** © 2023 by the authors. Licensee MDPI, Basel, Switzerland. This article is an open access article distributed under the terms and conditions of the Creative Commons Attribution (CC BY) license (<https://creativecommons.org/licenses/by/4.0/>).

## 1. Introduction

Miniaturized affinity monolith chromatography uses in situ synthesized monolithic supports (in, for example, fused silica capillaries), which are functionalized with biological targets such as proteins, receptors, antibodies or enzymes [1–5]. It is widely used for purification and enrichment in sample preparation [6–8], chiral separation [9] and the ligand or fragment screening in drug discovery [2,10–12]. Applications also include the study of biological interactions to provide information on the stoichiometry, thermodynamics and kinetics of the interaction between the immobilized biological target and ligands in solution [13,14]. Monolithic columns with inner diameters in the tens of  $\mu\text{m}$  range offer the tremendous advantage of reducing the amount of biological material to be immobilized.

Whatever the application, the underlying monolithic material supporting the biomolecules must meet two main criteria: the highest possible number of active proteins per unit volume and its intrinsic ability to limit non-specific interactions. The search for an inconspicuous support in affinity chromatography is a complex and difficult task [15,16]. For miniaturized affinity chromatography purposes, organic monoliths are usually widely used [12,17]. Indeed, the wide variety of commercially available monomers allows for the tuning of their surface properties and the tailoring of the available functional moieties for their subsequent grafting to a biological target [18]. Among the great variety of monoliths, poly(GMA-co-EDMA) monoliths have long been considered the gold standard [1], and they have found

applications in many fields [19]. In fact, they provide access to well-known and widely used types of biomolecule grafting (direct epoxy grafting, grafting after an epoxy ring opening into diol and the subsequent oxidation into aldehyde moieties).

Recently, we have shown (through a systematic study based on the retention behavior of a set of 41 test molecules) that non-specific interactions caused by these monolithic poly(GMA-co-EDMA)-based stationary phases are not negligible, regardless of the grafting process used [20]. Considering the hydrophobic nature of such interactions, we proposed the synthesis of a more hydrophilic monolith by replacing the EDMA crosslinker with a more hydrophilic one (N,N'-Methylenebis(acrylamide)). A more hydrophilic monolith with reduced-nonspecific interactions (for all solutes except cations) and a high-protein-grafting capacity was successfully obtained. However, we demonstrated that the epoxy ring opening step into diol moieties (in acidic mediums) leads to side reactions—i.e., the partial oxidation of acrylamide moieties into acidic ones—and it is responsible for the increase in non-specific interactions for cationic compounds. A hot-water-mediated hydrolysis was proposed at the expense of synthesis time (18 h instead of 1 h acid-catalyzed hydrolysis). In line with these ongoing efforts to optimize both the manufacturing and the performances of affinity nano-LC columns, we propose the synthesis of a new monolith by replacing the functional GMA monomer with 2,3-dihydroxypropyl methacrylate (DHPMA) to directly synthesize the diol monolith and suppress the time-consuming epoxy ring opening step (Figure 1). The preparation of hydrophilic monoliths using diol-based methacrylate monomers has been proposed with EDMA or PETA (pentaerythritol triacrylate) as crosslinkers, but the process has never been explored with the use of a more hydrophilic MBA [15,21,22].

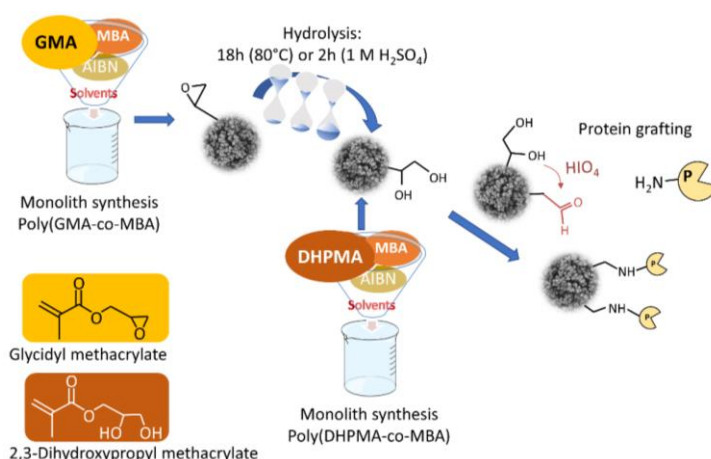


**Figure 1.** Schematic representation of the different steps of preparation of monolithic affinity columns from the poly(GMA-co-MBA) monolith and the time-saving poly(DHPMA-co-MBA) alternative.

Firstly, the synthesis parameters (polymerization mixture composition, temperature and polymerization time) were optimized to obtain a homogeneous monolith inside 75  $\mu\text{m}$  i.d. capillary columns, as well as to determine its main properties in terms of permeability, porosity, mean pore diameter and efficiency. We also demonstrated its ability to perform HILIC separations with a series of nucleoside test compounds. After the immobilization of proteins, the newly synthesized monolith was used for miniaturized affinity chromatography. The protein grafting capacity was assessed by determining the number of binding active sites present on the monolith surface after grafting biofunctionalization. Streptavidin was used as a model target protein and 4'-hydroxyazobenzene-2-carboxylic acid (HABA) as a test ligand. The non-specific interactions (in a pure aqueous medium as is used in affinity chromatography) were characterized using the previously developed methodology based on the systematic investigation of the retention behavior of a library of small chemical compounds. This set of compounds was selected to cover a wide range of physico-chemical characteristics. All these experiments were performed by frontal affinity experiments (with

a dedicated in-house-developed instrumentation [18]) as described in the Materials and Methods section. At last, the potential of this monolith was illustrated in weak affinity chromatography, where three Concanavalin ligands were retained and ranked according to decreasing  $K_d$  values.

## 2. Materials and Methods

### 2.1. Reagents and Buffers

Streptavidin (from *Streptomyces avidinii*, affinity purified,  $\geq 13$  U  $\text{mg}^{-1}$  of protein); Concanavalin A (Con A) (from *Canavalia ensiformis*); (3-methacryloxypropyl)-trimethoxysilane ( $\gamma$ -MAPS); ethylene dimethacrylate (EDMA); glycidyl methacrylate (GMA); acrylamide; N,N'-Methylenebis(acrylamide) (MBA); 1-propanol; 1,4-butanediol; dimethyl sulfoxide (DMSO); sodium periodate; lithium hydroxide; dipotassium hydrogen phosphate ( $\text{K}_2\text{HPO}_4$ ); o-phosphoric acid; sulfuric acid; sodium cyanoborohydride; triethylamine (TEA); azobis(isobutyronitrile) (AIBN); 4'-Hydroxyazobenzene-2-carboxylic acid (HABA); 4-nitrophenyl  $\alpha$ -D-mannopyranoside (PN-Man); 4-nitrophenyl  $\alpha$ -D-glucopyranoside (PNGlc); 4-nitrophenyl  $\alpha$ -D-galactopyranoside (PNGal); biotinylated Concanavalin A; and ligands (Table S1) were purchased from Sigma-Aldrich (L'Isle d'Abeau Chesne, France). Moreover, 2,3-Dihydroxypropyl methacrylate (DHPMA) was purchased from Polysciences (Hirschberg, Germany). All aqueous solutions were prepared using  $>18$  M $\Omega$  of deionized water. Phosphate buffer was prepared by dissolving 1.17 g of  $\text{K}_2\text{HPO}_4$  in 100 mL of ultrapure water, and the pH was adjusted to 7.4 with phosphoric acid.

### 2.2. Monolithic Capillary Column Synthesis

A total of 75  $\mu\text{m}$  of i.d. fused-silica capillaries with polyimide (TSP) coating were purchased from Cluzeau info Labo (Sainte-Foy-La-Grande, France). Capillary activation was conducted by flushing 15 cm length capillaries with a 5% ( $v/v$ ) solution of  $\gamma$ -MAPS in methanol/water (95/5,  $v/v$ ) and 2.5% TEA for 1 h at 7 bars. The capillaries were then rinsed with methanol for 15 min at 7 bar and dried at room temperature under a nitrogen stream before use.

#### 2.2.1. In-Capillary Poly(GMA-co-MBA) Monolith Synthesis

The poly(GMA-co-MBA) monoliths were prepared as follows [20]. First, a solvent mixture was prepared by mixing 3330 mg of DMSO, 1480 mg of 1,4-butanediol and 1850 mg of dodecanol. Then, 320 mg of MBA was added and sonicated for 1 h at room temperature. After dissolving the MBA, 480 mg of GMA was added and sonicated for 1 h at room temperature. A total of 8 mg of AIBN was added, and the final mixture was sonicated for 15 min at room temperature. The activated capillary (TSP capillary) was then filled with the polymerization mixture under 1 bar of  $\text{N}_2$  pressure and the ends of the capillary were sealed. The polymerization reaction was performed in a water bath at 57  $^\circ\text{C}$  for 18 h. After polymerization, the monoliths were rinsed with methanol for 1 h and kept wet until use.

#### 2.2.2. In-Capillary Poly(DHPMA-co-MBA) Monolith Synthesis

The poly(DHPMA-co-MBA) monoliths were prepared as follows. First, a mixture of solvents was prepared by mixing 888 mg of DMSO, 395 mg of 1,4-butanediol and 397 mg of dodecanol. Then, 80 mg of MBA was added and sonicated for 1 h at room temperature. After the dissolution of MBA, 120 mg of DHPMA were added and sonicated for 1 h at room temperature. A total of 2 mg of AIBN was added and the final mixture was sonicated for 15 min at room temperature. The activated capillary was filled with the polymerization mixture and sealed for polymerization in a water bath at 85  $^\circ\text{C}$  for various periods of time (as indicated in the text). After polymerization, the monoliths were rinsed with methanol for 1 h and kept wet until use.

### 2.3. Column Biofunctionalization

#### 2.3.1. Preparation of Streptavidin-Functionalized Monolithic Capillary Columns

The epoxy groups of the GMA-based monolith were hydrolyzed into diols either in an acidic medium (by flowing 1 M of sulfuric acid for 2 h) or in hot water (at 80 °C for 18 h), as has been previously reported [20]. The diol monolithic columns (hydrolyzed GMA-based and DHPMA-based monoliths) were subjected to a 0.12 M NaIO<sub>4</sub> solution at pH 5.5 for 1 h at 7 bars to oxidize the diol groups into aldehyde ones. Then, a 1 mg mL<sup>-1</sup> streptavidin solution and a 4 mg mL<sup>-1</sup> NaBH<sub>3</sub>CN solution in 67 mM of phosphate buffer (pH 6) were percolated through the column for 18 h at 7 bars at room temperature. After immobilization, the column was flushed with sodium borohydride (2.5 mg mL<sup>-1</sup> phosphate buffer, 67 mM, pH 8, for 2 h, 7 bar) to reduce the residual aldehydes. The streptavidin columns were then rinsed with phosphate buffer and stored at 4 °C.

The reduced aldehyde monolithic supports stand for the aldehyde columns were reduced with sodium borohydride (2.5 mg mL<sup>-1</sup> phosphate buffer, 67 mM, pH 8, for 2 h, 7 bar) without the protein grafting step.

#### 2.3.2. Preparation of Concanavalin a Monolithic Capillary Columns

The immobilization of concanavalin was conducted on streptavidin-functionalized monolithic capillary columns, which were used as generic columns by percolating a diluted solution of biotinylated Concanavalin A (the concentration was in the μM range in a 67 mM phosphate buffer, pH 7.4). The monitoring was achieved by in situ UV detection at the column outlet, which allowed for grafting to be stopped once the protein had passed through the column (breakthrough), i.e., once the column was saturated. Due to the dependence of Con A activity on the presence of calcium ions, before any use, the 67 mM phosphate buffer (enriched with Ca<sup>2+</sup> (67 mM K<sub>2</sub>HPO<sub>4</sub>, pH 7.4, 100 μM Ca<sup>2+</sup>)) was percolated through the column for at least 40 min to ensure the maximal activity of the immobilized Con A.

### 2.4. Nano-LC Experiments

Nano-LC chromatographic experiments (zonal or frontal mode) were carried out with a 7100 capillary electrophoresis Agilent system (Agilent Technologies, Waldbronn, Germany), which was equipped with an external pressure device (pressure up to 12 bars), and with the Chemstation software (Agilent). All experiments were carried out in “short-end” injection mode, with the inlet of the capillary immersed in the solution to be injected/infused. The UV detection was in situ achieved. A detection window was created by burning away the polyimide coating. The analyses were all carried out under a controlled room temperature of 25 °C. For the HILIC zonal analysis (separation of nucleosides and affinity separation of concanavalin ligands), the sample was hydrodynamically injected by applying a pressure at the inlet of the capillary (12 bars, 2 s).

Permeability was determined according to Darcy’s Law by measuring the dead time for a given pressure drop in a phosphate buffer mobile phase.

Total porosity was estimated after a determination of the hold-up time at a fixed-flow rate (300 nL min<sup>-1</sup>) using the Eksigent nanoLC 400 system (Sciex, Villebon-sur-Yvette, France) and Actipix<sup>TM</sup> in-capillary UV detection system (Paraytec, York, UK).

#### 2.4.1. Nano-FAC Experiments: Evaluation of Non-Specific Interactions

The non-specific interactions were evaluated by infusing test solutes individually (100 μM solutions in phosphate buffer, 67 mM, pH = 7.4) on the reduced aldehyde monolithic supports until the breakthrough time was reached. The columns were rinsed for 30 min in between each infusion. If non-specific interactions occurred, the solute was captured by the support until equilibrium was reached, and the breakthrough time  $t_{breakthrough}$  was delayed from the dead time.

$$q_{capt} = (t_{breakthrough} - t_0) \times F \times [L] = \frac{(t_{breakthrough} - t_0)}{t_0} \times V_0 \times [L] = k_{ns} \times V_0 \times [L]$$

where  $F$  is the flow rate to the dead time,  $V_0$  the dead volume of the column and  $k_{ns}$  the retention factor of the solute due to non-specific interactions.

#### 2.4.2. Quantification of the Number of Protein Active Binding Sites (Streptavidin or Concanavalin Columns)

To determine the number of streptavidin active binding sites that were available after grafting, HABA ( $K_d = 100 \mu\text{M}$ ) was percolated as a test solute with increasing concentrations (5, 10, 50, 100 and 200  $\mu\text{M}$  solutions were prepared in phosphate buffer, 67 mM, pH = 7.4) without a rinsing step between the percolations of the different concentrations (staircase experiments) [23]. The number of ligands captured in each step was determined, and the cumulative number of ligands captured was calculated by summing the number captured in all steps. The double reciprocal plot of the number of ligands captured versus the ligand concentration allowed for the simultaneous determination of both the  $K_d$  value of the target–ligand interaction and the number of available active sites ( $B_{act}$ ). The same set of experiments was performed with Concanavalin A columns to determine the number of concanavalin active binding sites. Solutions of 4-nitrophenyl  $\alpha$ -D-mannopyranoside (PNMan) ( $K_d = 40.9 \pm 6.2 \mu\text{M}$  [24] and 14–17  $\mu\text{M}$  [25,26]), prepared at 5 to 40  $\mu\text{M}$  in 20 mM of ammonium acetate buffer (pH 7.4) were percolated on the stationary phase and detected at 300 nm.

### 3. Results and Discussion

#### 3.1. Synthesis and Characterization of DHPMA-co-MBA Monoliths

The synthesis conditions of the poly(DHPMA-co-MBA) monoliths were based on our previous work on poly(GMA-co-MBA) monoliths. In this previous work, hydrophilic GMA-based monoliths were prepared using  $N,N'$ -methylenebis(acrylamide) (MBA) as the crosslinker to reduce non-specific interactions. In the present work, GMA was replaced by DHPMA to obtain the hydrophilic diol-functionalized monolith in one step, thus avoiding the time-consuming epoxy ring opening step. It should be emphasized that changing just one parameter, in this case the nature of the functionalized monomer, involves re-optimizing the synthesis. We kept the composition of the porogenic solvent constant and varied the temperature and the polymerization time to obtain homogeneous and uniform monolithic capillary columns (which were evaluated by visual inspection under a microscope) with a satisfactory permeability (in the range of  $10^{-14} \text{ m}^2$ ). The best synthesis conditions were obtained for a thermally initiated polymerization during 30 min at 85 °C with the polymerization mixture composition as shown in Table 1.

**Table 1.** Composition of the poly(DHPMA-co-MBA) polymerization mixture.

	Weight (mg)	%
DHPMA	120	6.38
MBA	80	4.26
AIBN	2	1 (of monomers)
DMSO	888	
1,4-butanediol	395	89.4
Dodecanol	397	

The permeability of the monolith was estimated according to Darcy's law in an 80/20 ( $v/v$ ) acetonitrile/water mobile phase at a pressure of 12 bar while using octylbenzene as the non-retained compound to determine the column dead time. The mean permeability, estimated over 23 columns prepared with three different polymerization mixtures (seven or eight columns per polymerization mixture) was  $(4.8 \pm 0.5) \times 10^{-14} \text{ m}^2$ . The low standard deviation showed that the synthesis was highly reproducible. The total

porosity, determined by measuring the hold-up time at a fixed flow rate of  $300 \text{ nL min}^{-1}$ , was  $85 \pm 2\%$ .

Knowing the permeability  $B^0$  and the total porosity  $\varepsilon_T$ , the Kozeny–Carman Equation (1) was used to calculate the size of the equivalent through the pores diameter ( $d_{pore}$ ) of the monolith [27]:

$$d_{pore} = 2 \left( \frac{5B^0}{\varepsilon_T} \right)^{\frac{1}{2}} \quad (1)$$

According to Equation (1),  $d_{pore}$  was estimated to  $1.2 \text{ }\mu\text{m}$ .

Finally, the efficiency of the monolith (8 cm in length) was evaluated at about  $9400 \pm 1300$  plates ( $n = 3$  columns) at the optimal linear flow velocity  $u_{opt}$  of  $0.09 \text{ cm s}^{-1}$  (i.e.,  $117,600$  plates/m at  $206 \text{ nL min}^{-1}$ ), which was achieved by using thiourea as a retained solute ( $k = 0.4$  at  $80/20$  (v/v) acetonitrile/water mobile phase composition (Figure 2)). These column kinetic performances with a high efficiency for an optimum flow rate close to  $0.1 \text{ cm s}^{-1}$  for organic monoliths are very interesting and are representative of the overall structural homogeneity of the monolith [28,29].

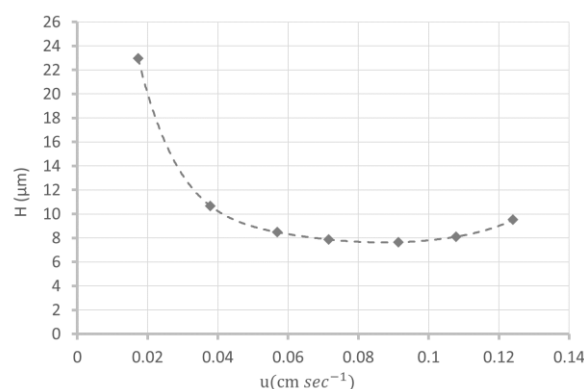


**Figure 2.** Van Deemter plot relating to the theoretical plate height to the mobile phase velocity on a poly(DHPMA-co-MBA) monolithic column ( $L = 8 \text{ cm}$ ,  $i.d = 75 \mu\text{m}$ ) in an  $80/20$  (v/v) acetonitrile/water mobile phase.

To confirm the highly hydrophilic character of the monolith, its ability to separate compounds in the HILIC mode was evaluated, as illustrated Figure 3, with the separation of five nucleosides. The elution order was indicative of a HILIC separation mechanism and clearly reflects the highly hydrophilic nature of this new poly(DHPMA-co-MBA) monolithic stationary phase. Compared to commercial columns, such as Acquity BEH Amide and Atlantis premier BEH ZIC-HILIC (Waters), the order between uridine and adenosine was reversed, whereas the retention factor of cytosine was quite the same ( $k = 3.08$  on the Acquity BEH amide and  $k = 2.5$  for our monolith, with a  $90/10$  acetonitrile/water mobile phase).

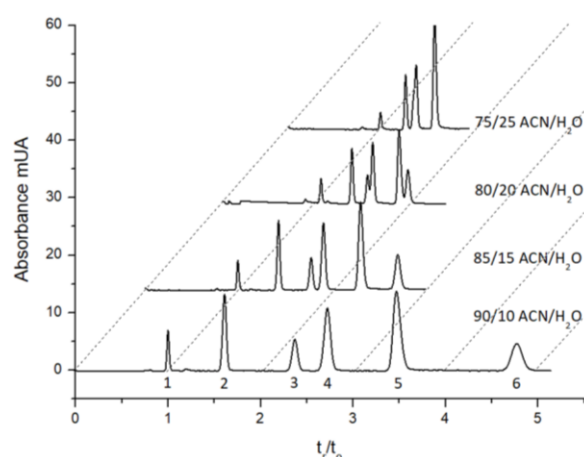


**Figure 3.** Chromatograms showing the separation of five nucleosides on an 8 cm length poly(DHPMA-co-MBA) monolith (75  $\mu\text{m}$  i.d.) for different mobile phase compositions. UV detection at 260 nm. Solutes were as follows: (1) octylbenzene as the dead time marker, (2) uracil, (3) uridine, (4) adenosine, (5) cytosine and (6) cytidine.

### 3.2. Characterization of the Number of Active Binding Sites after Protein Immobilization

In affinity chromatography, the number of active binding sites per unit volume is a critical parameter because it determines the total capacity of the affinity support (in the case of high-affinity enrichment/purification) and the range of detectable affinity (in the case of weak affinity chromatography). The higher the number of active binding sites per unit volume, the higher the capacity and the wider the range of detectable affinity. The number of active binding sites of the newly synthesized poly(DHPMA-co-MBA) monoliths ( $13 \pm 0.7 \text{ pmol cm}^{-1}$ ) was determined by frontal affinity chromatography, with streptavidin as the protein and HABA as the ligand ( $K_d = 100 \text{ }\mu\text{M}$ ) (Figure S1). This protein (used here as model protein) was also used in affinity chromatography to prepare the generic columns on which any type of biotinylated target protein can be quantitatively captured thanks to the high-affinity streptavidin–biotin interaction. The number of active protein binding sites was in the same order of magnitude as that obtained with poly(GMA-co-MBA) monolithic capillary columns that are subjected to either acid hydrolysis ( $13 \pm 0.8 \text{ pmol cm}^{-1}$ ) or thermal treatment in hot water at  $80 \text{ }^\circ\text{C}$  for 18 h ( $16 \pm 0.8 \text{ pmol cm}^{-1}$ ), but with a shortened synthesis procedure instead. In fact, this monolith was obtained with a shorter polymerization time (30 min, instead of overnight) and one less step (from 2 to 18 h depending on the hydrolysis mode). Thus, the poly(DHPMA-co-MBA) monolith is a good alternative to the poly(GMA-co-MBA) one.

### 3.3. Evaluation of the Non-Specific Interactions on Poly(DHPMA-co-MBA) Monoliths and Comparison with Poly(GMA-co-MBA) Monoliths

The evaluation of non-specific interactions was performed on “reduced aldehyde monoliths”. In fact, reduced aldehydes are the remaining functions after biomolecule grafting and subsequent reductions in residual aldehyde functions that remain on the monolith surface. To evaluate non-specific interactions on the reduced aldehyde poly(DHPMA-co-MBA) monolith, we used the same methodology and the same set of 41 small molecules previously used to characterize the poly(GMA-co-MBA) monoliths [20]. This set of molecules (selected from a library of small ligand molecules, called fragments, used in the preliminary affinity screening step in fragment-based drug discovery) covers a wide range of physicochemical properties in terms of net charge,  $\log_D$ , H-bond donors and acceptors. The physicochemical properties and chemical structures of this set of fragments are detailed in Table S1. The retention factor of each solute (measured in a pure buffered aqueous buffer solution as in affinity experiments) was compared with those measured on reduced aldehyde poly(GMA-co-MBA) monoliths that were subjected to either acid hydrolysis or thermal

treatment in hot water (Figure 4). In fact, we have shown that the rapid acidic-mediated epoxy ring opening was accompanied by side reactions (the partial hydrolysis of amide functions into carboxylic acid ones) leading to a specific behavior of cationic compounds whose non-specific interactions greatly increased at the end of this step. If this partial hydrolysis can be greatly reduced by hot water hydrolysis (a reduction in non-specific interactions of cationic compounds), then it is at the expense of the hydrolysis time (18 h instead of 2 h), i.e., the total preparation time.

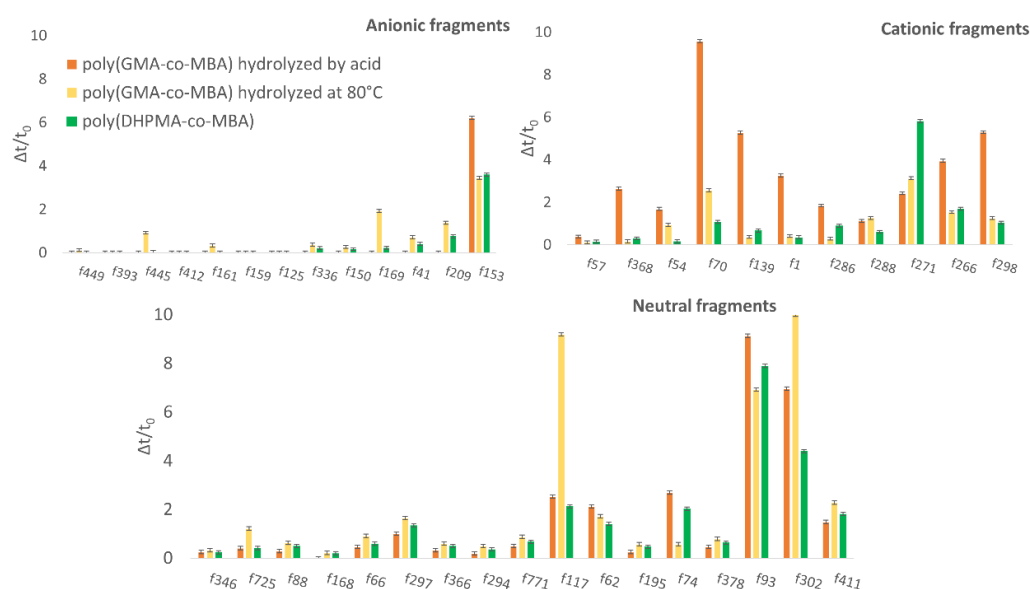


**Figure 4.** Bar graphs of the retention factors for the 41 molecules (classified according to their global charge: anionic, cationic or neutral fragments) in the reduced aldehyde poly(GMA-co-MBA) \* monolith hydrolyzed in acid media (orange), the reduced aldehyde poly(GMA-co-MBA) \* monolith hydrolyzed in hot water (yellow) and the aldehyde-reduced poly(DHPMA-co-MBA) \* monolith.

For all compounds, with a few exceptions (f271, f286, f93 and f74) for unknown reasons, the non-specific interactions measured on the DHPMA-co-MBA monoliths were comparable or even significantly lower (f54, f70, f288, f169, f41, f209, f275, f66 and f302) than those measured on the aldehyde-reduced GMA-co-MBA monoliths, regardless of the hydrolysis method used (acid or hot water mediated). Replacing the GMA monomer with a diol monomer (DHPMA) eliminated the time-consuming epoxy ring opening step and associated side reactions, such as partial hydrolysis of acrylamide moieties into acidic ones. It is clear from these results that this monolith offers a real added value in terms of preparation time.

Finally, the stability of this DHPMA-co-MBA monolith in a pure aqueous medium (acetate buffer, 20 mM pH = 7.4) was evaluated. The retention factors remained constant over the period of use (one week of continuous use), and even after 3 additional months of storage (the column was stored in an aqueous solution at room temperature and kept wet).

### 3.4. Separation of Concanavalin Ligands by Weak Affinity Chromatography

On a streptavidin-functionalized monolithic capillary column used as a generic column, a biotinylated Concanavalin A (Con A) solution was percolated until saturation of the column was achieved. Indeed, the immobilization of Con A by the streptavidin–biotin interaction was very stable, quantitative and instantaneous. After immobilization, the number of active Con A binding sites was evaluated at  $66 \pm 2$  pmol with PNMan as a test solute. Figure 5 illustrates the separations of three compounds on a column before and after immobilization of Con A. The non-specific interactions of all compounds on the monolithic column before Con A immobilization were weak (a retention factor close

to 0.3 for each compound), as shown in the chromatogram in Figure 5A. On the other hand, on the Con A monolithic column (Figure 5B), the compounds were separated in order of increasing affinity (decreasing  $K_d$ ). Indeed, Con A was known to bind the mannose residue in glycoprotein. Furthermore, 4-nitrophenyl  $\alpha$ -D-mannopyranoside (PNMan) with a  $K_d$  value of about 40  $\mu$ M was the most retained compound, whereas 4-nitrophenyl  $\alpha$ -D-galactopyranoside, which has no specific interaction with Con A, was not retained. Moreover, the 4-nitrophenyl  $\alpha$ -D-glucopyranoside with a  $K_d$  value  $> 200 \mu$ M [25] was intermediate. The high density of active sites makes it possible to detect an affinity as low as  $K_d > 200 \mu$ M. These columns are therefore suitable for a search of low-affinity ligands, particularly in the scope of fragment-based drug discovery.

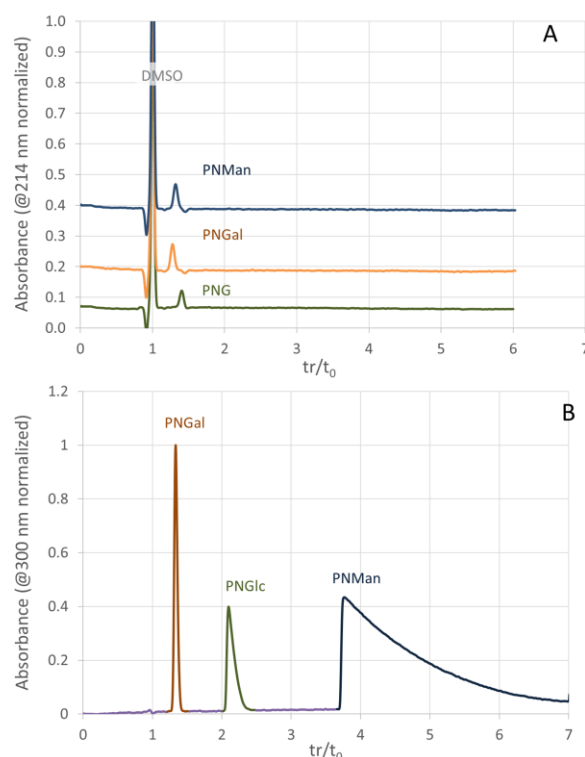


**Figure 5.** Chromatograms of the different 4-nitrophenyl  $\alpha$ -D-glycopyranosides on poly(DHPMA-co-MBA) monolithic capillary columns before (A) and after (B) Concanavalin A immobilization. Solutes were as follows: 4-nitrophenyl  $\alpha$ -D-galactopyranoside (PNGal), 4-nitrophenyl  $\alpha$ -D-glucopyranoside (PNGlc) and 4-nitrophenyl  $\alpha$ -D-glycopyranoside (PNMan). DMSO was used as the dead time marker.

#### 4. Conclusions

Optimizing the underlying support of affinity columns to reduce non-specific interactions while favoring high biomolecule grafting capacity and reducing synthesis time is an ongoing goal. In this work, we developed the one-step synthesis of a diol organic monolith to replace the gold-standard epoxy organic monoliths (which must be hydrolyzed prior to use). The suppression of the epoxy ring opening step, as well as the short polymerization time (30 min) allowed for a drastic reduction in the synthesis time since hot water-mediated hydrolysis is a time-consuming step. The resulting monolith offers high permeability ( $(4.8 \pm 0.5) \times 10^{-14} \text{ m}^2$ ), high efficiency (117,600 plates/m) and minimized non-specific interactions. The separation of nucleosides illustrates its potential in the HILIC mode, and the retention data set of the 41 test substances shows a drastic reduction in non-specific interactions. The protein grafting capacity was also greatly improved ( $13 \pm 0.7 \text{ pmol cm}^{-1}$  instead of  $8 \pm 0.3 \text{ pmol cm}^{-1}$  for the GMA-co-EDMA gold-standard monolith). All these results highlight the added value of this new monolith in the field of miniaturized affinity chromatography.

**Supplementary Materials:** The following supporting information can be downloaded at <https://www.mdpi.com/article/10.3390/separations10080437/s1>, Table S1: presents the list of physicochemical properties of the tests solutes to evaluate the non-specific interactions on monolithic columns. Figure S1 and the related text illustrate the graphical plots that allow for the obtained compounds by nano-frontal affinity chromatography, as well as the data processing that allows for the columns' characterization (protein-specific interactions (active binding sites, affinity (dissociation constant)) and non-specific interactions).

**Author Contributions:** J.G.: Conceptualization, Methodology, Validation, Formal analysis and Writing—original draft. G.P.: Investigation and Visualization. A.D.: Investigation and Visualization. F.-X.V.: Investigation and Visualization. C.D.: Conceptualization, Methodology, Validation, Supervision, Writing—original draft, Writing—review and Project administration. V.D.: Conceptualization, Methodology, Writing—review and editing and Supervision. All authors have read and agreed to the published version of the manuscript.

**Funding:** The authors acknowledge the support of the French Agence Nationale de la Recherche (ANR) under grant ANR-21-CE29-0012 (project NanoWAC).

**Data Availability Statement:** Data sharing not applicable.

**Conflicts of Interest:** The authors declare no conflict of interest.

## References

1. Pfaunmiller, E.L.; Paulemond, M.L.; Dupper, C.M.; Hage, D.S. Affinity Monolith Chromatography: A Review of Principles and Recent Analytical Applications. *Anal. Bioanal. Chem.* **2013**, *405*, 2133–2145. [[CrossRef](#)] [[PubMed](#)]
2. Calleri, E.; Temporini, C.; Massolini, G. Frontal Affinity Chromatography in Characterizing Immobilized Receptors. *J. Pharm. Biomed. Anal.* **2011**, *54*, 911–925. [[CrossRef](#)] [[PubMed](#)]
3. Rodriguez, E.L.; Poddar, S.; Iftekhar, S.; Suh, K.; Woolfork, A.G.; Ovbude, S.; Pekarek, A.; Walters, M.; Lott, S.; Hage, D.S. Affinity Chromatography: A Review of Trends and Developments over the Past 50 Years. *J. Chromatogr. B* **2020**, *1157*, 122332. [[CrossRef](#)] [[PubMed](#)]
4. Hage, D.S. Affinity Chromatography: A Review of Clinical Applications. *Clin. Chem.* **1999**, *45*, 593–615. [[CrossRef](#)]
5. Alla, A.J.; Stine, K.J. Recent Strategies for Using Monolithic Materials in Glycoprotein and Glycopeptide Analysis. *Separations* **2022**, *9*, 44. [[CrossRef](#)]
6. Salim, H.; Pero-Gascon, R.; Giménez, E.; Benavente, F. On-Line Coupling of Aptamer Affinity Solid-Phase Extraction and Immobilized Enzyme Microreactor Capillary Electrophoresis-Mass Spectrometry for the Sensitive Targeted Bottom-Up Analysis of Protein Biomarkers. *Anal. Chem.* **2022**, *94*, 6948–6956. [[CrossRef](#)]
7. Espina-Benitez, M.B.; Randon, J.; Demesmay, C.; Dugas, V. Development and Application of a New In-Line Coupling of a Miniaturized Boronate Affinity Monolithic Column with Capillary Zone Electrophoresis for the Selective Enrichment and Analysis of Cis-Diol-Containing Compounds. *J. Chromatogr. A* **2017**, *1494*, 65–76. [[CrossRef](#)]
8. Pero-Gascon, R.; Benavente, F.; Minic, Z.; Berezovski, M.V.; Sanz-Nebot, V. On-Line Aptamer Affinity Solid-Phase Extraction Capillary Electrophoresis-Mass Spectrometry for the Analysis of Blood  $\alpha$ -Synuclein. *Anal. Chem.* **2020**, *92*, 1525–1533. [[CrossRef](#)]
9. Pfaunmiller, E.L.; Hartmann, M.; Dupper, C.M.; Soman, S.; Hage, D.S. Optimization of Human Serum Albumin Monoliths for Chiral Separations and High-Performance Affinity Chromatography. *J. Chromatogr. A* **2012**, *1269*, 198–207. [[CrossRef](#)]
10. Temporini, C.; Massolini, G.; Marucci, G.; Lambertucci, C.; Buccioni, M.; Volpini, R.; Calleri, E. Development of New Chromatographic Tools Based on A2A Adenosine Receptor Subtype for Ligand Characterization and Screening by FAC-MS. *Anal. Bioanal. Chem.* **2013**, *405*, 837–845. [[CrossRef](#)]
11. Lecas, L.; Hartmann, L.; Caro, L.; Mohamed-Bouteben, S.; Raingeval, C.; Krimm, I.; Wagner, R.; Dugas, V.; Demesmay, C. Miniaturized Weak Affinity Chromatography for Ligand Identification of Nanodiscs-Embedded G-Protein Coupled Receptors. *Anal. Chim. Acta* **2020**, *1113*, 26–35. [[CrossRef](#)]
12. Lecas, L.; Randon, J.; Berthod, A.; Dugas, V.; Demesmay, C. Monolith Weak Affinity Chromatography for Mg-Protein-Ligand Interaction Study. *J. Pharm. Biomed. Anal.* **2019**, *166*, 164–173. [[CrossRef](#)] [[PubMed](#)]
13. Hage, D.S.; Chen, J. Quantitative Affinity Chromatography: Practical Aspects. In *Handbook of Affinity Chromatography*; CRC Press: Boca Raton, FL, USA, 2006; pp. 596–628.
14. Kasai, K. Frontal Affinity Chromatography: An Excellent Method of Analyzing Weak Biomolecular Interactions Based on a Unique Principle. *Biochim. Biophys. Acta-Gen. Subj.* **2021**, *1865*, 129761. [[CrossRef](#)] [[PubMed](#)]
15. Gunasena, D.N.; El Rassi, Z. Hydrophilic Diol Monolith for the Preparation of Immuno-Sorbents at Reduced Nonspecific Interactions. *J. Sep. Sci.* **2011**, *34*, 2097–2105. [[CrossRef](#)] [[PubMed](#)]
16. Khadka, S.; El Rassi, Z. Postpolymerization Modification of a Hydroxy Monolith Precursor. Part III. Activation of Poly(Hydroxyethyl Methacrylate-Co-Pentaerythritol Triacrylate) Monolith with Epoxy Functionalities Followed by Bonding of Glycerol, Polyamines, and Hydroxypropyl- $\beta$ -Cyclodextrin for Hydrophilic Interaction and Chiral Capillary Electrochromatography. *Electrophoresis* **2016**, *37*, 3178–3185. [[CrossRef](#)] [[PubMed](#)]

17. Poddar, S.; Sharmeen, S.; Hage, D.S. Affinity Monolith Chromatography: A Review of General Principles and Recent Developments. *Electrophoresis* **2021**, *42*, 2577–2598. [[CrossRef](#)] [[PubMed](#)]
18. Svec, F. Porous Polymer Monoliths: Amazingly Wide Variety of Techniques Enabling Their Preparation. *J. Chromatogr. A* **2010**, *1217*, 902–924. [[CrossRef](#)]
19. Li, Z.; Rodriguez, E.; Azaria, S.; Pekarek, A.; Hage, D.S. Affinity Monolith Chromatography: A Review of General Principles and Applications. *Electrophoresis* **2017**, *38*, 2837–2850. [[CrossRef](#)]
20. GIL, J.; Krimm, I.; Dugas, V.; Demesmay, C. Preparation of Miniaturized Hydrophilic Affinity Monoliths: Towards a Reduction of Non-Specific Interactions and an Increased Target Protein Density. *J. Chromatogr. A* **2023**, *1687*, 463670. [[CrossRef](#)]
21. Jancó, M.; Xie, S.; Peterson, D.S.; Allington, R.W.; Svec, F.; Fréchet, J.M.J. Effect of Porosity and Surface Chemistry on the Characterization of Synthetic Polymers by HPLC Using Porous Polymer Monolithic Columns. *J. Sep. Sci.* **2002**, *25*, 909–916. [[CrossRef](#)]
22. Selvaraju, S.; El Rassi, Z. Tandem Lectin Affinity Chromatography Monolithic Columns with Surface Immobilised Concanavalin A, Wheat Germ Agglutinin and Ricinus Communis Agglutinin-I for Capturing Sub-Glycoproteomics from Breast Cancer and Disease-Free Human Sera. *J. Sep. Sci.* **2012**, *35*, 1785–1795. [[CrossRef](#)] [[PubMed](#)]
23. Gottardini, A.; Netter, C.; Dugas, V.; Demesmay, C. Two Original Experimental Setups for Staircase Frontal Affinity Chromatography at the Miniaturized Scale. *Anal. Chem.* **2021**, *93*, 16981–16986. [[CrossRef](#)] [[PubMed](#)]
24. Gray, R.D.; Glew, R.H. The Kinetics of Carbohydrate Binding to Concanavalin A. *J. Biol. Chem.* **1973**, *248*, 7547–7551. [[CrossRef](#)] [[PubMed](#)]
25. Oda, Y.; Kasai, K.; Ishii, S. Studies on the Specific Interaction of Concanavalin A and Saccharides by Affinity Chromatography. Application of Quantitative Affinity Chromatography to a Multivalent System. *J. Biochem.* **1981**, *89*, 285–296. [[CrossRef](#)]
26. Ohyama, Y.; Kasai, K.; Nomoto, H.; Inoue, Y. Frontal Affinity Chromatography of Ovalbumin Glycoasparagines on a Concanavalin A-Sepharose Column. A Quantitative Study of the Binding Specificity of the Lectin. *J. Biol. Chem.* **1985**, *260*, 6882–6887. [[CrossRef](#)]
27. Skudas, R.; Grimes, B.A.; Thommes, M.; Unger, K.K. Flow-through Pore Characteristics of Monolithic Silicas and Their Impact on Column Performance in High-Performance Liquid Chromatography. *J. Chromatogr. A* **2009**, *1216*, 2625–2636. [[CrossRef](#)]
28. Svec, F. Quest for Organic Polymer-Based Monolithic Columns Affording Enhanced Efficiency in High Performance Liquid Chromatography Separations of Small Molecules in Isocratic Mode. *J. Chromatogr. A* **2012**, *1228*, 250–262. [[CrossRef](#)]
29. Aydoğan, C.; Beltekin, B.; Demir, N.; Yurt, B.; El Rassi, Z. Nano-Liquid Chromatography with a New Monolithic Column for the Analysis of Coenzyme Q10 in Pistachio Samples. *Molecules* **2023**, *28*, 1423. [[CrossRef](#)]

**Disclaimer/Publisher’s Note:** The statements, opinions and data contained in all publications are solely those of the individual author(s) and contributor(s) and not of MDPI and/or the editor(s). MDPI and/or the editor(s) disclaim responsibility for any injury to people or property resulting from any ideas, methods, instructions or products referred to in the content.